

Ligand-based transport resonances of single-molecule magnet spin filters: Suppression of the Coulomb blockade and determination of the orientation of the magnetic easy axis

Fatemeh Rostamzadeh Renani¹ and George Kirczenow¹

¹*Department of Physics, Simon Fraser University, Burnaby, British Columbia, Canada V5A 1S6*

(Dated: November 1, 2018)

We investigate single molecule magnet transistors (SMMTs) with ligands that support transport resonances. We find the lowest unoccupied molecular orbitals of Mn₁₂-benzoate SMMs (with and without thiol or methyl-sulfide termination) to be on ligands, the highest occupied molecular orbitals being on the Mn₁₂ magnetic core. We predict gate controlled switching between Coulomb blockade and coherent resonant tunneling in SMMTs based on such SMMs, strong spin filtering by the SMM in both transport regimes, and that if such switching is observed then the magnetic easy axis of the SMM is parallel to the direction of the current through the SMM.

PACS numbers: 75.50.Xx, 85.75.-d, 85.65.+h, 73.23.Hk

Charge and spin transport through individual molecules bridging a pair of electrodes, and through single-molecule transistors that include a third “gate” electrode, have been studied intensively for more than a decade.¹ Because of their large magnetic anisotropy barriers and associated stable magnetic moments,² single molecule magnets (SMMs) raise the possibility of molecular spintronic devices and molecular magnetic information storage.³ Therefore, at present, the transport properties of transistors based on individual SMMs are attracting considerable experimental⁴⁻⁶ and theoretical⁴⁻¹² interest.³ Models based on effective spin-Hamiltonians⁴⁻⁸ and density functional theory (DFT)-based calculations⁹⁻¹² have yielded many important insights into the transport properties of these systems. However, in the theoretical transport studies to date the organic ligands that surround the magnetic cores of the SMMs have received limited attention: The focus has been on SMMs in which the lowest unoccupied molecular orbital (LUMO) and the highest occupied molecular orbital (HOMO) are both on the SMM’s magnetic core. Thus the ligands have acted as simple tunnel barriers that hinder electron transmission between the electrodes and the magnetic core. In the case of weak tunneling, the electrostatic energy associated with charging of the core states during transport suppresses electrical conduction at low source-drain and gate voltages.^{1,3} This phenomenon is known as Coulomb blockade and has been observed in SMM transport experiments.⁴⁻⁶

In this paper we explore theoretically the electron and spin transport in SMMs in which we predict the ligands to play a more active and interesting role: We consider Mn₁₂-benzoate [Mn₁₂O₁₂(O₂CC₆H₅)₁₆(H₂O)₄, abbreviated Mn₁₂-Ph] SMMs with and without terminating methyl-sulfide or thiol groups. For these SMMs we predict the lowest unoccupied molecular orbital (LUMO), and orbitals nearby in energy, to be *on ligands*, and the highest occupied molecular orbital (HOMO) and orbitals nearby in energy to be on the SMM’s magnetic core. We also predict that, for certain geometries of these SMMs thiol-bonded to gold electrodes, some molecular orbitals that are close in energy to the LUMO hybridize strongly with the gold electrodes. It follows that for these bonding geometries transport via these near-LUMO orbitals should *not* be subject to Coulomb blockade, unlike transport via the HOMO. As we explain below SMM transis-

tors in which such bonding geometries are realized can readily be identified experimentally by carrying out measurements of the electric current versus source-drain and gate voltage such as are routinely performed in single-molecule transistor experiments today. Furthermore, for SMM transistors identified in this way we predict the molecular easy axis to be approximately parallel to the direction of current flow. Thus the present theory provides a *practical* way to use standard *non-spin-resolved* current measurements to determine the orientation of the SMM magnetic easy axis, over which there was no control in SMM transistor experiments to date. Moreover, we predict these *magnetically oriented* SMM transistors to be *effective spin filters* at low and moderate source-drain voltages.

The results that we present are based on the semi-empirical extended Hückel tight-binding model of quantum chemistry that we generalize in this paper to include spin polarization and spin-orbit coupling. For Mn₁₂ SMMs (both neutral molecules and negatively charged ions) the present model yields results consistent with experiment for the total spin of the SMM, for the spins of the individual Mn ions, for the direction of the magnetic easy axis, for the size of the magnetic anisotropy barrier (MAB), for the size of the molecular HOMO-LUMO gap and for the spins of the HOMO and LUMO states.¹³ The overall degree of agreement with experiment obtained with the present model is comparable to or better than that achieved with DFT calculations corrected by inclusion of the adjustable Hubbard U parameter.^{9,10} However, calculations based on the present model are much less compute intensive than those based on DFT. Thus, we are able to study transport in larger molecules than are readily accessible to DFT computations and therefore, unlike in previous theoretical studies, to include complete sets of ligands none of which have been shortened or replaced by hydrogen atoms.

Our SMM Hamiltonian is $H^{\text{SMM}} = H^{\text{EH}} + H^{\text{spin}} + H^{\text{SO}}$. Here H^{EH} is the extended Hückel Hamiltonian.^{1,14,15} The spin Hamiltonian H^{spin} gives rise to the magnetic polarization of the molecule. Spin orbit coupling is described by H^{SO} .

In extended Hückel theory the basis is a small set of Slater-type atomic valence orbitals $|\Psi_{i\alpha}\rangle$; $|\Psi_{i\alpha}\rangle$ is the i^{th} orbital of the α^{th} atom. The diagonal elements of H^{EH} are the experimentally determined negative valence orbital ionization energies ε_i , $\langle \Psi_{i\alpha} | H^{\text{EH}} | \Psi_{i\alpha} \rangle = H_{i\alpha;i\alpha}^{\text{EH}} = \varepsilon_{i\alpha}$.

The non-diagonal matrix elements are assumed to be proportional to the orbital overlaps $D_{i\alpha;i'\alpha'} = \langle \Psi_{i\alpha} | \Psi_{i'\alpha'} \rangle$, i.e., $H_{i\alpha;i'\alpha'}^{\text{EH}} = D_{i\alpha;i'\alpha'} K \frac{\varepsilon_{i\alpha} + \varepsilon_{i'\alpha'}}{2}$, where K is chosen empirically for consistency with experimental molecular electronic structure data. In our calculations,¹⁵ as in Ref. 14, $K = 1.75 + \Delta_{i\alpha;i'\alpha'}^2 - 0.75\Delta_{i\alpha;i'\alpha'}^4$ where $\Delta_{i\alpha;i'\alpha'} = \frac{\varepsilon_{i\alpha} - \varepsilon_{i'\alpha'}}{\varepsilon_{i\alpha} + \varepsilon_{i'\alpha'}}$.

For non-magnetic systems, transport calculations based on extended Hückel theory have yielded elastic^{16,17} and inelastic¹⁸ conductances in agreement with experiment for molecules thiol-bonded to gold electrodes and have also explained transport phenomena observed in scanning tunneling microscopy (STM) experiments on molecular arrays on silicon¹⁹ as well as electroluminescence data²⁰, current-voltage characteristics²⁰ and STM images²¹ of molecules on complex substrates.

The extended Hückel Hamiltonian H^{EH} does not describe spin polarization whereas in the Mn_{12} SMMs the four inner and eight outer Mn ions are spin polarized with antiparallel spins. In our model, H^{spin} addresses this issue. We define its matrix elements $\langle i s \alpha | H^{\text{spin}} | i' s' \alpha' \rangle = H_{i s \alpha; i' s' \alpha'}^{\text{spin}}$ between valence orbitals i and i' of atoms α and α' with spin s and s' by

$$H_{i s \alpha; i' s' \alpha'}^{\text{spin}} = D_{i\alpha;i'\alpha'} (\mathcal{A}_{i\alpha} + \mathcal{A}_{i'\alpha'}) \langle s | \hat{n} \cdot \mathbf{S} | s' \rangle / (2\hbar)$$

$$\mathcal{A}_{i\alpha} = \begin{cases} \mathcal{A}_{\text{inner}} & \text{for inner Mn } d\text{-valence orbitals} \\ \mathcal{A}_{\text{outer}} & \text{for outer Mn } d\text{-valence orbitals} \\ 0 & \text{otherwise} \end{cases} \quad (1)$$

Here \hat{n} is a unit vector aligned with the magnetic moment of the SMM, and \mathbf{S} is the one-electron spin operator. $\mathcal{A}_{\text{inner}}$ and $\mathcal{A}_{\text{outer}}$ are parameters chosen so that in the Mn_{12} ground state the spin of each inner (outer) Mn is $S_{\text{inner(outer)}} \cong -\frac{3}{2} (+2)$.

Spin-orbit coupling is also not included in extended Hückel theory.^{1,14,15} However, it is responsible for the magnetic anisotropy of SMMs. We therefore generalize extended Hückel theory to include spin-orbit coupling by evaluating approximately the matrix elements of the spin-orbit coupling Hamiltonian H^{SO} starting from the standard expression²² $H^{\text{SO}} = \boldsymbol{\sigma} \cdot \nabla V(\mathbf{r}) \times \mathbf{p} / (2mc)^2$ where \mathbf{p} is the momentum operator, $V(\mathbf{r})$ is the electron Coulomb potential energy, $\boldsymbol{\sigma} = (\sigma_x, \sigma_y, \sigma_z)$ and σ_x, σ_y and σ_z are the Pauli spin matrices. We approximate $V(\mathbf{r})$ by a sum of atomic potential energies $V(\mathbf{r}) \simeq \sum_{\alpha} V_{\alpha}(\mathbf{r} - \mathbf{r}_{\alpha})$ where \mathbf{r}_{α} is the position of α^{th} atomic nucleus. Noting that the spin-orbit coupling arises mainly from the atomic cores where the potential energy $V_{\alpha}(\mathbf{r} - \mathbf{r}_{\alpha})$ is approximately spherically symmetric, yields $H^{\text{SO}} \simeq \sum_{\alpha} \frac{1}{2m^2c^2} \frac{1}{|\mathbf{r} - \mathbf{r}_{\alpha}|} \frac{dV_{\alpha}(|\mathbf{r} - \mathbf{r}_{\alpha}|)}{d|\mathbf{r} - \mathbf{r}_{\alpha}|} \mathbf{S} \cdot \mathbf{L}_{\alpha}$ where $\mathbf{S} = \hbar\boldsymbol{\sigma}/2$, $\mathbf{L}_{\alpha} = (\mathbf{r} - \mathbf{r}_{\alpha}) \times \mathbf{p}$ is the orbital angular momentum operator with respect to the position of the α^{th} nucleus and the sum is over all atoms α . Evaluating the matrix elements of H^{SO} between valence orbitals i and i' of atoms α and α' with spin s and s' we then find

$$\langle i s \alpha | H^{\text{SO}} | i' s' \alpha' \rangle \simeq E_{i s i' s'; \alpha}^{\text{SO}} \delta_{\alpha\alpha'} + (1 - \delta_{\alpha\alpha'}) \sum_j (D_{i\alpha;j\alpha'} E_{j s i' s'; \alpha'}^{\text{SO}} + [D_{i' \alpha'; j\alpha} E_{j s' i s; \alpha}^{\text{SO}}]^*) \quad (2)$$

The first term on the right-hand side is the intra-atomic contribution, the remaining terms are the inter-atomic contribution

and

$$E_{i s i' s'; \alpha}^{\text{SO}} = \langle \alpha, l_i, d_i, s | \mathbf{S} \cdot \mathbf{L}_{\alpha} | \alpha, l_i, d_i, s' \rangle \times \langle R_{\alpha, l_i} | \frac{1}{2m^2c^2} \frac{1}{|\mathbf{r} - \mathbf{r}_{\alpha}|} \frac{dV(|\mathbf{r} - \mathbf{r}_{\alpha}|)}{d|\mathbf{r} - \mathbf{r}_{\alpha}|} | R_{\alpha, l_i} \rangle \delta_{l_i l_{i'}} \quad (3)$$

where the atomic orbital wave function $\Psi_{i\alpha}$ has been expressed as the product of a radial wave function R_{α, l_i} and directed atomic orbital $|\alpha, l_i, d_i, s\rangle$. Here l_i is the angular momentum quantum number and d_i may be $s, p_x, p_y, p_z, d_{xy}, d_{xz}, \dots$ depending on the value of l_i . In Eq. (3) the matrix elements of $\mathbf{S} \cdot \mathbf{L}_{\alpha}$ are evaluated as in Ref. 23 while the radial integrals are the spin-orbit coupling constants.

We estimate the magnetic anisotropy energy of the SMM from the total ground state energy expression $E_{\text{total}} = \sum_i E_i - \sum_i \langle \phi_i | H^{\text{spin}} | \phi_i \rangle / 2$ where E_i and $|\phi_i\rangle$ are eigenenergies and eigenstates of H^{SMM} and the summations are over all occupied states. Since H^{spin} represents electron-electron interactions at a mean field level, the second summation on the right hand side is required to avoid double counting the corresponding interaction energy.

Experimental estimates²⁴ of the spin-orbit coupling constant for Mn d -orbitals have been in the range 0.023–0.051 eV, while theoretical estimates²⁵ have been in the range 0.038–0.055 eV. In this paper for Mn atoms we use the value 0.036 eV, which is consistent with the experimental and theoretical values. We find that the spin-orbit coupling constants of the other atoms do not affect the SMMs' properties significantly and that the intra- and inter-atomic terms in Eq. (2) make contributions of the same order of magnitude to the magnetic anisotropy barriers of Mn_{12} SMMs. In this work the values of $H_{i\alpha;i'\alpha'}^{\text{EH}}$ and $D_{i\alpha;i'\alpha'}$ that enter the extended Hückel model, Eqs. (1) and (2), were adopted without change from Refs. 14 and 15. The molecular geometries that we studied were based on the experimentally measured geometry²⁶ of Mn_{12} -Ph modified as necessary by adding thiol or methyl sulfide groups to the ligands. Thus the only free parameters in the present theory are the $\mathcal{A}_{i\alpha}$ of Eq. (1) that control the spin polarizations of the Mn atoms; we chose $\mathcal{A}_{\text{inner}} = 3.0$ eV and $\mathcal{A}_{\text{outer}} = -3.5$ eV. For these parameter values in the Mn_{12} -Ph ground state we find the inner and outer Mn ions to have spins -1.6 and 1.99 , the SMM to have a total spin of 10 and the calculated MAB to be 2.50 meV, all consistent with experiment.^{26,27}

The calculated densities of states projected on the inner and outer Mn atoms, and carbon atoms of Mn_{12} -Ph are shown in Fig. 1. The HOMO and nearby levels are on the outer Mn and are filled with spin-up electrons (parallel to the total spin), consistent with $S_{\text{outer}} = +2$. The occupied inner Mn states are filled with spin-down electrons consistent with $S_{\text{inner}} = -\frac{3}{2}$. The carbon atoms are weakly spin polarized. The calculated HOMO-LUMO energy gap is ~ 0.7 eV. (Note that experimental and theoretical estimates for the Mn_{12} family range from a few tenths of an electron Volt to more than 1 eV.^{10,12,28}) As is seen in Fig. 1, our calculation predicts the LUMO of Mn_{12} -Ph to be mainly on the carbon atoms of the ligands. There is at this time no *direct* experimental evidence as to whether the LUMO of Mn_{12} -Ph is located on the ligands as in Fig. 1 or on the Mn_{12} core of the molecule. However, experimental

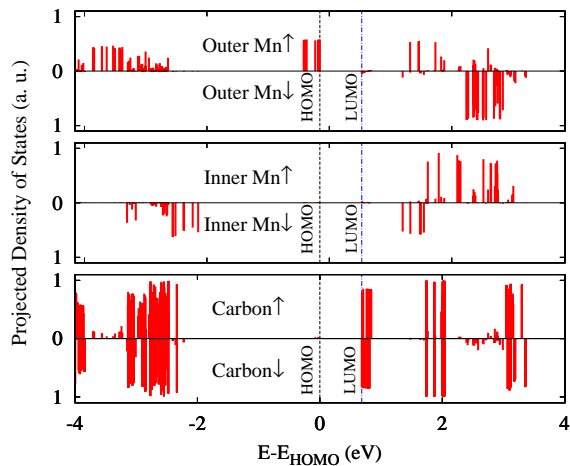


Figure 1. Projected density of states for majority (spin-up) and minority (spin-down) electrons on Mn and carbon atoms for the isolated Mn_{12} -Ph molecule without thiol or methylsulfide end groups.

measurements of the MAB carried out on the neutral²⁷ and negatively charged²⁹ Mn_{12} -Ph species yielded values of 3.3 and 2.41 meV, respectively, a difference of only 27%. Since the main source of the MAB of Mn_{12} is the Jahn-Teller distortion of the Mn_{12} core of the molecule⁵ this insensitivity of the MAB to the oxidation state of the molecule is consistent with the added electron of the negatively charged species residing mainly on the ligands rather than on the Mn_{12} core, as one might expect if the LUMO of the neutral molecule is on the ligands as in Fig. 1. Our calculations also predict only a small change in the MAB when an electron is added to the neutral Mn_{12} -Ph molecule, since in our model the added electron locates primarily on the ligands rather than the magnetic molecular core. Our prediction that the LUMO is on the ligands (i.e. the benzoate groups, including both their carbon and oxygen atoms) and not on the Mn_{12} core is also consistent with the large 3.3–3.6 eV electron affinity of the benzoate species.^{30,31}

The ligands of SMMs that are studied in transport experiments with gold electrodes are normally thiolated and we shall therefore focus our attention on Mn_{12} -Ph-Th, i.e., Mn_{12} -Ph terminated with methyl sulfide (SCH_3) groups, the methyl be-

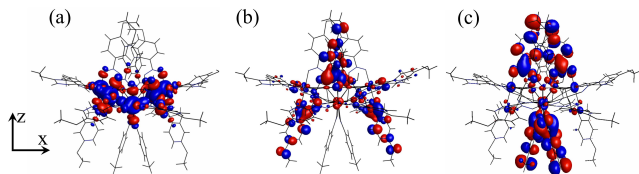


Figure 2. Wave functions for Mn_{12} -Ph-Th (a) spin-up HOMO (b) spin-down LUMO (c) spin-up orbital near LUMO in energy. The magnetic easy axis and total molecular spin are parallel to the z -axis. Although the LUMO and near LUMO orbitals are mainly on the ligands they are spin polarized due to their small but non-zero overlaps with the magnetic core of the molecule that are visible in (b) and (c).

ing displaced by gold when the molecule bonds to the contacts. The calculated densities of states of Mn_{12} -Ph-Th (and of Mn_{12} -Ph with thiol end groups) projected on the Mn and C atoms are similar to those shown in Fig. 1 for Mn_{12} -Ph. The locations and spins of the HOMO and LUMO and of orbitals close to these in energy are also similar for Mn_{12} -Ph with and without thiol or methyl sulfide end groups. The calculated HOMO, LUMO and another representative molecular orbital close in energy to the LUMO are shown in Fig. 2 for Mn_{12} -Ph-Th. The HOMO is located on the magnetic core of the molecule. However, the LUMO and molecular orbitals close in energy to the LUMO are located on ligands, and specifically on those ligands that are oriented approximately parallel to the magnetic easy axis of the molecule which points in the z -direction in Fig. 2. This finding has important implications for electron and spin transport in Mn_{12} -Ph-Th-based SMM transistors: The HOMO and molecular orbitals close in energy to the HOMO have very little overlap with any of the ligands. Therefore *all* of the ligands that couple the molecule to the contacts act as strong tunnel barriers for transport mediated by the HOMO and molecular orbitals nearby in energy. For this reason transport via the HOMO and molecular orbitals close in energy to the HOMO is predicted to display the classic signature of Coulomb blockade. By contrast if any gold contact bonds to a ligand on which certain molecular orbitals close in energy to the LUMO (for example, that in Fig. 2(c)) have a strong presence, those molecular orbitals will hybridize strongly with the gold contact and therefore transport via that molecular orbital (or orbitals) will not be subject to Coulomb blockade. Furthermore, because these orbitals occupy ligands that are oriented approximately parallel to the molecular easy axis as in Fig. 2, if such transport that is not subject to Coulomb blockade is observed experimentally, then the molecule must be oriented relative to the gold contacts in such a way that the magnetic easy axis is approximately parallel to the direction of current flow through the molecule. We note that although there have been theoretical suggestions previously of possible ways to determine the orientation of the easy axis in a SMM transistor,^{8,12} these suggestions have been difficult to implement in practice and no experimental control over the orientation of the easy axis in SMM transistors has been achieved experimentally to date. The present theory is much more promising in this regard since the experimental observation of the presence or absence of Coulomb

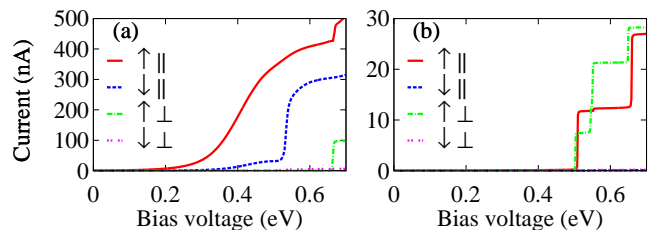


Figure 3. Calculated spin resolved current parallel (\parallel) and perpendicular (\perp) to the easy axis for (a) positive and (b) negative gate voltage vs. bias voltage at zero temperature. The gate potential at the molecule = +0.2 and -0.2V in (a) and (b), respectively.

blockade in single-molecule transistors is currently carried out routinely, and we predict that if Coulomb blockade is observed at negative gate voltages (transport via the HOMO and nearby states) but not at positive gate voltages (transport via the LUMO or nearby states) then the easy axis is approximately parallel to the direction of current flow.

Our transport calculations based on Landauer theory and the Lippmann-Schwinger equation³² predict Mn₁₂-Ph-Th-based SMM transistors with gold contacts to be effective spin filters at low source-drain bias for both positive and negative gate voltages. Representative results for a Mn₁₂-Ph-Th molecule bonded to gold contacts *via ligands on which near-LUMO orbitals have a strong presence* (and therefore the current through the SMM is roughly parallel to the magnetic easy axis) are shown in Fig. 3. Here mainly spin-up electrons are transmitted through the SMM at low bias for both positive (Fig. 3(a)) and negative (Fig. 3(b)) gate voltages. The *gradual* rise of the current with bias voltage (from ~ 0.2 to ~ 0.67 V) in Fig. 3(a) is a direct manifestation of the large broadening of the near-LUMO molecular orbitals responsible for transport that is due to the strong hybridization of those orbitals with the gold contacts that also suppresses Coulomb blockade for positive gate bias. By contrast, the *abrupt* step-like rise to much lower values of the current for negative gate voltages (Fig. 3(b)) is due to the near-HOMO molecular orbitals being very weakly coupled to the gold contacts and therefore being only very weakly broadened, they are subject to Coulomb blockade.³⁶ For molecules bonded to gold electrodes via ligands that are roughly perpendicular to the easy axis, neither near-LUMO nor near-HOMO orbitals have significant presence on the ligands, see Fig. 2. Thus, for geometries with a current through the SMM that is roughly perpendicular to the magnetic easy axis, the ligands act as strong tunnel barriers for both positive and negative gate voltages (Fig. 3). Coulomb blockade is therefore predicted for *both* signs of the gate voltage.

In conclusion, previous studies of transport in single molecule magnets have considered the situation where the HOMO and LUMO both reside on the magnetic core of the molecule. Here we have proposed that this need not always be the case, Mn₁₂ benzoate with and without termi-

nating methyl-sulfide or thiol groups being a possible example. We have predicted that for these systems the LUMO and molecular orbitals close in energy to the LUMO reside on the organic ligands that are oriented approximately parallel to the magnetic easy axis of the molecule and that when the molecule bonds via these ligands to gold electrodes in a single-molecule transistor, transport via some of the near-LUMO orbitals should *not* be in the Coulomb blockade regime. For other orientations of the molecule transport via the LUMO and near-LUMO orbitals is predicted to be in the Coulomb blockade regime, as is transport via the HOMO and near-HOMO orbitals for all molecular orientations. This effect should make it possible to study experimentally the transport in single molecule magnet transistors that behave as spin filters and in which the orientation of the magnetic easy axis relative to the electrodes is known. In single-molecule magnet transistor experiments to date the orientation of the magnetic easy axis has not been determined although it controls the spin polarization of the current in such devices.

While this work has focused on Mn₁₂ benzoate and its derivatives, we expect other single molecule magnets with LUMO and/or HOMO states located on the ligands to exist as well due to the small HOMO-LUMO gaps exhibited by a variety of organic molecules that may be chosen as ligands. For example it is well established that polyacetylene and polythiophene have HOMO-LUMO gaps of 1.4 eV³⁷ and 0.85 eV³⁸, respectively. Both of these are smaller than the experimentally measured energy gap (~ 1.8 eV)³⁹ between the highest occupied and lowest unoccupied orbitals localized on the cores of the Mn₁₂ molecules. It is reasonable to expect oligomers (consisting of several monomers) derived from these polymers to have similarly small HOMO-LUMO gaps. If such oligomers are used as ligands for Mn₁₂ SMMs contacted with gold electrodes, the gold Fermi level is expected to lie within the oligomer HOMO-LUMO gap and also within the HOMO-LUMO gap of the Mn₁₂ core. Therefore either the HOMO or the LUMO (or both) of the Mn₁₂ SMM with such ligands is expected to lie on the ligands.

This research was supported by CIFAR, NSERC, Westgrid and Compute Canada. We thank B. Gates and B. L. Johnson for helpful comments and discussions.

¹ For a recent review see G. Kirichenow, in *The Oxford Handbook of Nanoscience and Technology, Volume I: Basic Aspects*, edited by A. V. Narlikar and Y. Y. Fu, (Oxford University Press, Oxford, U.K. 2010), Chap. 4.
² D. Gatteschi, R. Sessoli, and J. Villain, *Molecular Nanomagnets* (Oxford University Press, New York, 2006).
³ L. Bogani and W. Wernsdorfer, *Nature Mater.* **7**, 179 (2008)
⁴ H. B. Heersche *et al.*, *Phys. Rev. Lett.* **96**, 206801 (2006).
⁵ M.-H. Jo *et al.*, *Nano Lett.* **6**, 2014 (2006).
⁶ A. S. Zyazin *et al.*, *Nano Lett.* **10**, 3307 (2010).
⁷ G.-H. Kim and T.-S. Kim, *Phys. Rev. Lett.* **92**, 137203 (2004); C. Romeike, M. R. Wegewijs, H. Schoeller, *Phys. Rev. Lett.* **96**, 196805 (2006); C. Timm, and F. Elste, *Phys. Rev. B* **73**, 235304 (2006); M. Miśniorny, I. Weymann, J. Barnas, *Phys. Rev. B* **79**, 224420 (2009); H.-Z. Lu, B. Zhou, and S.-Q. Shen, *Phys. Rev. B* **79**, 174419 (2009); F. Elste, C. Timm, *Phys. Rev. B* **81**, 024421 (2010).

⁸ C. Timm, *Phys. Rev. B* **76**, 014421 (2007).
⁹ S. Barraza-Lopez, K. Park, V. García-Suárez and J. Ferrer, *J. Appl. Phys.* **105**, 07E309 (2009); *Phys. Rev. Lett.* **102**, 246801 (2009).
¹⁰ C. D. Pemmaraju, I. Rungger, S. Sanvito, *Phys. Rev. B* **80**, 104422 (2009).
¹¹ Ł. Michalak, C. M. Canali, M. R. Pederson, M. Paulsson, and V. G. Benza, *Phys. Rev. Lett.* **104**, 017202 (2010).
¹² K. Park, S. Barraza-Lopez, V. M. García-Suárez, and J. Ferrer, *Phys. Rev. B* **81**, 125447 (2010).
¹³ The results of our systematic studies for members of the Mn₁₂ SMM family other than Mn₁₂-Ph-Th will be presented elsewhere.
¹⁴ J. H. Ammeter *et al.*, *J. Am. Chem. Soc.* **100**, 3686 (1978).
¹⁵ The YAEHMOP code implementation of the extended Hückel theory (Ref. 14) by G. A. Landrum and W. V. Glassey (Source-Forge, Fremont, California, 2001) was used. YAEHMOP does not include spin-orbit coupling.
¹⁶ S. Datta *et al.*, *Phys. Rev. Lett.* **79**, 2530 (1997); E. G. Emberly, G. Kirichenow, *Phys. Rev. Lett.* **87**, 269701 (2001); *Phys. Rev. B* **64**, 235412

- (2001); J.G. Kushmerick *et al.*, Phys. Rev. Lett. **89**, 086802 (2002).
- ¹⁷ D. M. Cardamone and G. Kirczenow, Phys. Rev. B **77**, 165403 (2008).
- ¹⁸ F. Demir and G. Kirczenow, J. Chem. Phys. **134**, 121103 (2011).
- ¹⁹ G. Kirczenow *et al.*, Phys. Rev. B **72**, 245306 (2005); Phys. Rev. B **80**, 035309(2009); P. G. Piva *et al.*, Phys. Rev. Lett. **101**, 106801 (2008).
- ²⁰ J. Buker and G. Kirczenow, Phys. Rev. B **78**, 125107 (2008).
- ²¹ J. Buker and G. Kirczenow, Phys. Rev. B **72**, 205338 (2005).
- ²² See C. Kittel, *Quantum Theory of Solids* (Wiley, New York, 1963), p. 181.
- ²³ S. Kunschuh, M. Gmitra, J. Fabian, Phys. Rev. B **82**, 245412 (2010).
- ²⁴ *CRC Handbook of Chemistry and Physics*, 68th ed., edited by D. R. Lide (CRC Press, Boca Raton, FL, 1987–1988); J. Bendix, M. Brorson, and C. E. Schaffer, Inorg. Chem. **32**, 2838-2849 (1993); M. Gerloch, *Orbitals, Terms and States* (Wiley, Chichester, 1986).
- ²⁵ F. Herman and S. Skillman, *Atomic Structure Calculations* (Prentice-Hall, Inc., Englewood Cliffs, N. J., 1963); E. Francisco and L. Pueyo, Phys. Rev. B **37**, 5278(1988); M. Vijayakumar, M. S. Gopinathan, J. Mol. Struct.: THEOCHEM **361**, 15 (1996); E. Francisco and L. Pueyo, Phys. Rev. A **36**, 1978 (1987); A. Abragam and B. Bleaney, *Electron Paramagnetic Resonance of Transition Ions* (Clarendon Press, Oxford, U.K., 1970).
- ²⁶ S. M. J. Aubin *et al.*, Inorg.Chem. **40**, 2127 (2001).
- ²⁷ K. Takeda, K. Awaga, and T. Inabe, Phys. Rev. B **57**, R11062 (1998).
- ²⁸ J. M. North *et al.*, Phys. Rev. B **67**, 174407 (2003); D. W. Boukhvalov *et al.*, Phys. Rev. B **75**, 014419 (2007).
- ²⁹ K. Takeda, K. Awaga, Phys. Rev. B **56**, 14560 (1997).
- ³⁰ H.-K Woo, X.-B Wang, B. Kiran, L.-S Wang, J. Phys. Chem. A **109**, 11395 (2005).
- ³¹ Since the LUMO is located on the whole benzoate group, the appropriate electron affinity to consider is that of the benzoate group rather than that of the benzene molecule.
- ³² The methodology used has been described in Refs. [17](#), [19](#), [33–35](#).
- ³³ G. Kirczenow, Phys. Rev. B **75**, 045428 (2007).
- ³⁴ H. Dalglish and G. Kirczenow, Nano Lett. **6** 1274 (2006).
- ³⁵ H. Dalglish and G. Kirczenow, Phys. Rev. B **72**, 155429 (2005).
- ³⁶ The calculation in Fig.3(b), in common with those based on DFT,^{9,10,12} does not include Coulomb blockade, but still provides information regarding the energy level broadening due to hybridization between the molecular orbitals and gold leads that controls whether Coulomb blockade occurs.
- ³⁷ C. R. Fincher, *et al.*, Phys. Rev. B **20**, 1589 (1979).
- ³⁸ K. Lee, G. K. Sotzing, Macromolecules **34**, 5746 (2001).
- ³⁹ S. Voss, M. Fonin, U. Rudiger, M. Burgert, U. Groth, Appl. Phys. Lett. **90**, 133104 (2007)